



Front-face and right-angle fluorescence spectroscopy for monitoring EVOO evolution

N. Hernández-Sánchez, L. Lleó, B. Diezma, Faten Ammari, T.R. Cuadrado, P. Barreiro, Jean-Michel Roger, M. Ruiz Altisent

► To cite this version:

N. Hernández-Sánchez, L. Lleó, B. Diezma, Faten Ammari, T.R. Cuadrado, et al.. Front-face and right-angle fluorescence spectroscopy for monitoring EVOO evolution. VIII International Olive Symposium, Oct 2016, Split, Croatia. pp.497-503, 10.17660/ActaHortic.2018.1199.79 . hal-02608025

HAL Id: hal-02608025

<https://hal.inrae.fr/hal-02608025>

Submitted on 16 May 2020

HAL is a multi-disciplinary open access archive for the deposit and dissemination of scientific research documents, whether they are published or not. The documents may come from teaching and research institutions in France or abroad, or from public or private research centers.

L'archive ouverte pluridisciplinaire **HAL**, est destinée au dépôt et à la diffusion de documents scientifiques de niveau recherche, publiés ou non, émanant des établissements d'enseignement et de recherche français ou étrangers, des laboratoires publics ou privés.

Front-face and right-angle fluorescence spectroscopy for monitoring EVOO evolution

N. Hernández-Sánchez¹, L. Lleó¹, B. Diezma¹, F. Ammari², T.R. Cuadrado, P. Barreiro¹, J.M. Roger² and M. Ruiz-Altisent¹

¹Physical Properties Laboratory and Advanced Technologies in Agrifood, LPF-Tagralia, ETSIAAB, Universidad Politécnica de Madrid, Madrid, Spain

²Irstea, UMR ITAP, 361 Rue J.F. Breton, Montpellier Cedex 5, France

Abstract

Fluorescence spectroscopic techniques have been applied in a study in order to monitor the evolution of the spectral pattern of Extra Virgin Olive Oil (EVOO) samples exposed to indirect light at room temperature. Detailed information has been extracted from three dimensional Front-Face (FF) fluorescence spectra with excitation wavelengths ranging from 230 to 646 nm and emission wavelengths ranging from 250 to 698.5 nm. Relevant emission regions have been revealed in FF experiments that have been useful to study the variability of the characteristic spectral patterns and to develop fast inspection procedures. Such procedures include simultaneous excitation at the wavelengths lower than 400 nm, which has been proposed and implemented in a right-angle prototype in order to monitor the evolution of EVOO samples exposed to indirect light. Emission signals at local maxima around 400 nm, 434 nm, 464 nm, 513 nm and 674 nm are found relevant. Ongoing research highlights that hyperspectral images provide spectral patterns of the olives allowing a more precise sorting into categories, which would enable the classification into lots of oils with more homogeneous characteristics for subsequent modelling.

Keywords: Oil quality, oil storage, oxidation, principal component analysis

INTRODUCTION

The olive oil is spreading all over the world promoted by the sensorial attributes and health benefits associated with the chemical and nutritional composition of the extra virgin olive oil (EVOO) (López-Miranda et al., 2010). Under oxidation inducing conditions promoted by illumination, a sample of olive oil might contain a plethora of oxidation compounds. Most of the olive oil components involved in the oxidation processes, such as chlorophyll, antioxidants compounds (polyphenols and α -tocopherol), and primary and secondary oxidation products are fluorescent molecules (Sikorska et al., 2012). Thus, a complex fluorescence spectral pattern is expected to reveal the oxidation status. Fast inspection procedures are of great interest. Hence, identification of the bands of excitation wavelengths providing information on oxidation evolution is a major issue to develop a fast procedure with simultaneous excitation that give rise to the useful emission signals.

The present work shows the preliminary results of a study where detailed regions of excitation-emission wavelengths have been extracted from three dimensional front-face (FF) fluorescence spectra. Simultaneous excitation at the wavelengths of interest has been proposed and implemented in a right-angle (RA) prototype in order to monitor the evolution of EVOO samples exposed to indirect light.

The hyperspectral imaging system allows integrating spectroscopic and imaging techniques to enable direct identification of different components or quality characteristics

and their spatial distribution within the tested samples (Lara et al., 2013; Lleó et al., 2011). Hyperspectral imaging techniques have emerged as a powerful technique in agricultural and food systems as they overcome the limits of spectroscopic techniques and vision techniques, they. Hyperspectral images could provide detailed spectral patterns useful to characterize olives and to sort them into homogeneous categories previous to oil extraction.

MATERIALS AND METHODS

Samples

Set 1 included two EVOO samples directly obtained from producers (P1 and P2) and five EVOO samples (according to commercial labelling) acquired from retail markets (C1, C2, C3, C6 and C8); and seven olive oil (OO#) samples from retail markets (Table 1). 3D FF and RA fluorescence spectra were obtained from each sample, and then, analyzed and compared in order to assess the most suitable configuration of the right-angle experiments.

Table 1. Characteristics of the extra virgin olive oil and olive oil samples of Set 1 analyzed by 3D front-face and right-angle fluorescence spectroscopy.

EVOO Samples	P1	P2	C1	C2	C3	C6	C8
Cultivar	Arbequina	Picual	Arbequina	Hojiblanca	Picual	Blend: Hojiblanca Arbequina Picual Cornicabra	Arbequina
Origin	Producers	Producers	Retail market	Retail market	Retail market	Retail market	Retail market
K270	0.11	0.12	0.12	0.13	0.14	0.14	0.13
OO Samples	OO1	OO2	OO3	OO4	OO5	OO6	OO7
Origin	Retail market	Retail market	Retail market	Retail market	Retail market	Retail market	Retail market
K270	0.28	0.34	0.41	0.41	0.41	0.48	0.50

Set 2 included thirteen EVOO samples, according to commercial labelling, obtained from retail markets. Commercial samples (C#) included monovarietal oils, known varietal blends and unknown varietal blends (Table 2). These samples were exposed to indirect light in transparent glass bottles at room temperature during five months. RA fluorescence spectra were monthly acquired from each sample from the control month at the beginning of the experiment to the fifth month under treatment. Principal component analysis (PCA) was performed on centred data.

Table 2. Characteristics of the EVOO samples of Set 2 obtained at retail markets analyzed by right-angle fluorescence spectroscopy. (*, analyzed by 3D FF).

Sample	C1*	C2*	C3*	C4	C5	C6*	
Cultivar	Arbequina	Hojiblanca	Picual	Blend	Blend	Blend: Hojiblanca Arbequina Picual Cornicabra	
Sample	C7	C8*	C9	C10	C11	C12	C13
Cultivar	Blend: Hojiblanca Arbequina Picual Cornicabra	Arbequina	Blend	Blend	Blend	Blend	Blend

Set 3 included olive fruits samples, cultivar Picual, visually sorted into group 1 (G1: green and 'pintonas' olives), G2 (purple olives) and G3 (black olives).

Three-dimensional front-face fluorescence spectroscopy

Three-dimensional front-face (3D FF) fluorescence spectra were measured using a spectrofluorometer (LS45, Perkin-Elmer) equipped with a Xenon lamp source, excitation and emission monochromators and a front-face sample-cell holder.

The excitation wavelengths ranged from 230 to 646 nm (step 4 nm) and the emission wavelengths ranged from 250 to 698.5 nm (step 0.5 nm). Excitation and emission monochromator slit widths were set at 10 nm. Quartz cuvettes (10 mm × 10 mm × 45 mm) were filled with the oil samples without prior preparation.

For each olive oil sample a rectangular area was selected that included the region of oxidation products. The excitation band ranged from 274 nm to 400 nm and the emission band ranged from 375 to 550 nm. The coefficient of variation (CV) of the signal intensity was computed at every pair (ex_i, em_j) among the samples in both the EVOO group and the OO group.

For each excitation wavelength, the excitation spectrum was obtained as the sum of the signal along the selected emission wavelengths. The emission spectrum was obtained as the sum of the signal along the selected excitation wavelengths for each emission wavelength. Univariate and multivariate analyses were developed in order to identify the emission wavelengths with potential information related to K_{270} . The univariate approach consisted of the computation of the coefficient of determination R^2 between the signal intensity at each individual wavelength from 275 to 550 nm and the analytical K_{270} values. The multivariate approach computed the b-coefficients of a partial least square regression (PLSR) for the whole wavelengths range. Performance was evaluated through R^2 and the bias corrected standard error of prediction (SEP_c).

Right-angle fluorescence spectroscopy

The RA fluorescence spectra were obtained using a photonic multi-channel spectrometer (Hamamatsu, Japan) with detection wavelengths ranging from 196.9 nm to 958.8 nm (step 0.75 nm). A UV-VIS light source (L10290, Hamamatsu, Japan) was used with a Deuterium lamp, with spectral range from 200 to 400 nm. Integration time was set to 1400 ms and 3 repetitions per measurements were averaged.

A prototype with a right-angle sample-cell holder was designed and assembled by LPF-TAGRALIA. Two optical filters were coupled to the setup so as to constrain both the excitation and the emission wavelength ranges. The optical filter coupled with the fiber coming from light source allowed a beam with wavelengths below 400 nm. The other optical filter limits the registered beam to wavelengths higher than 400 nm. Measurements were carried out using quartz cuvettes (10 mm × 10 mm × 45 mm) directly on the oil samples without prior preparation.

Hyperspectral vision

The hyperspectral vision system consists of a push-broom CCD camera (Andor Luca) equipped with a spectrograph Headwall Photonics Hyperspec™ VNIR (400 to 1000 nm, 189 wavelengths, spectral resolution 3.17 nm). The illumination was provided by two halogens lamps. The platform moved under the camera and the image was scanned line by line according to the movement (push-broom system). The spatial resolution was 260 μm . Once the raw images were acquired, the corresponding relative reflectance hypercube was computed, containing the relative reflectance spectrum of each pixel of the image with respect to a reference (mean spectrum of a barium sulfate white reference). Standard Normal Variate and Savitsky Golay were pre-processing techniques applied to the spectra.

RESULTS AND DISCUSSION

Fluorescence spectroscopy

For each olive oil sample of Set 1 a rectangular area was selected that included the region of oxidation products. The excitation band ranged from 274 nm to 400 nm and the emission band ranged from 375 to 550 nm. Examples are shown in Figure 1.

The CV(%) of the signal intensity was computed at every pair (ex_i, em_j) among the samples in the corresponding group. For EVOO samples the region with the highest CV(%) values appeared within ex_i from 274 to 318 nm and em_j from 380 to 490 nm, i.e. CV higher than 25% up to 40% (red and dark yellow in Figure 1). Smaller regions showed CV around 25% (light yellow in Figure 1) and a large region showed values around 15% (light blue in Figure 1).

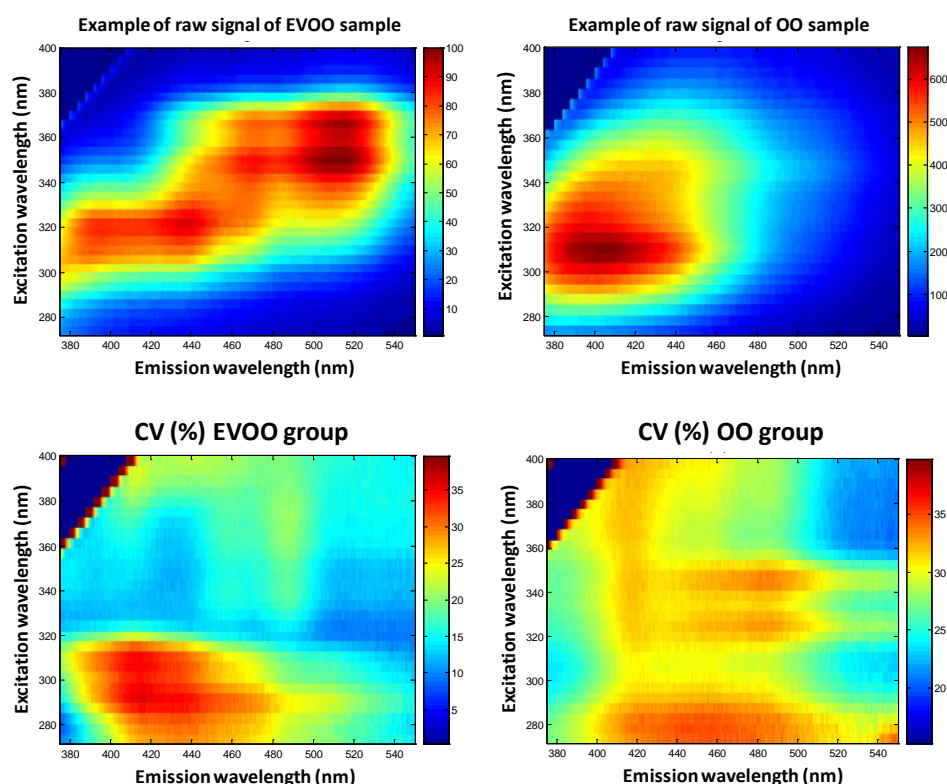


Figure 1. Upper left: Example of raw signal from 3D FF spectrum of an EVOO sample. Bottom left: Coefficient of variation (%) for the group of EVOO samples. Upper right: Example of raw signal from 3D FF spectrum of an OO sample. Bottom right: Coefficient of variation (%) for the group of OO samples. Note different colour scales.

For OO samples higher CV values were found than for EVOO samples. Most of the points within the selected area showed CV higher than 30% (Figure 1). Excitation wavelengths around 280, 325 and 345 nm provided wide emission ranges with the highest CV values, around 35%.

According to that, the sources of information on the oxidation conditions probably arise at least from these three excitation spectral regions. Therefore, a more complete evaluation relies on the registration of the signal resulting of wide bands of excitation wavelengths. When fast monitoring is additionally required, the optimal solution is to implement a simultaneous excitation at those wavelengths.

Another approach was considered by simulating a simultaneous excitation by summing the emission signal along the excitation wavelengths. Two spectral analyses, univariate and multivariate, were developed on emission spectra in order to identify the emission wavelengths with potential information related to K_{270} . Olive oil (OO) samples were included so as to increase the range of K_{270} values.

For the EVOO group low R^2 values were obtained, below 0.4, along the whole range. Despite that, two relevant wavelengths can be identified as corresponding to spectral peaks, i.e. around 375 nm and 443.5 nm, the former with the highest R^2 (Figure 2 upper left). As for the OO group, R^2 values higher than 0.7 were obtained at 400 nm and subsequent wavelengths for the whole range. When the grand group was analysed (EVOO and OO), R^2 reached values above 0.9 for all the wavelengths, with a maximum of 0.98 around 445 nm (Figure 2 upper left). The high R^2 for all the emission wavelengths suggests that an intense oxidation produces a general increase of the signal along the whole spectrum, which is related to the overall increase of K_{270} value. Signal from secondary oxidation products seems to dominate the whole spectra, probably concealing other signals.

The multivariate approach identifies a specific emission band ranging from 375 to 450 nm that provides higher b-coefficients, with a maximum around 410 nm (Figure 2 upper right). The R^2 was 0.94 and the SEP_c was 0.0364 using one latent variable.

In Figure 2 (bottom left) the intensity of the emission signal at 400 nm is depicted versus the measured K_{270} values. In Figure 2 (bottom right) similar result is obtained when multivariate prediction is illustrated by measured K_{270} values versus predicted K_{270} values for one latent variable.

The obtained results are similar to those found by previous works where a single excitation wavelength was used for excitation. Kyriadiakis and Skarkalis (2000) used 365 nm as excitation wavelength and found a R^2 of 0.96 between emission at 445 nm and K_{270} . Guzmán et al. (2015) found the best performance by applying PLSR with six latent variables for excitation wavelength at 380 nm. Emission spectra ranged from 300 to 800 nm. The root mean square prediction error was 0.08 and the R^2 was 0.92 obtained with the external validation.

However, in the present work a broad band of excitation wavelengths is studied with the aim of capturing signal arising from wider variety of compounds.

In view of these results, the signal arising from most of the fluorophores related to the oxidation processes could be obtained with excitation at wavelengths below 400 nm. The emission signals would be related to oxidation by-products and chlorophylls. A wide range of excitation would allow capturing different compounds undergoing production and degradation processes. Therefore, subsequent analyses focused on a simultaneous excitation of olive oil samples exposed to indirect light in a RA prototype.

From two months onwards, samples became a light yellowish/yellowish-brown fluid with solid material deposited at the bottom of the containers and minor variation in the spectral pattern was detected (results not shown).

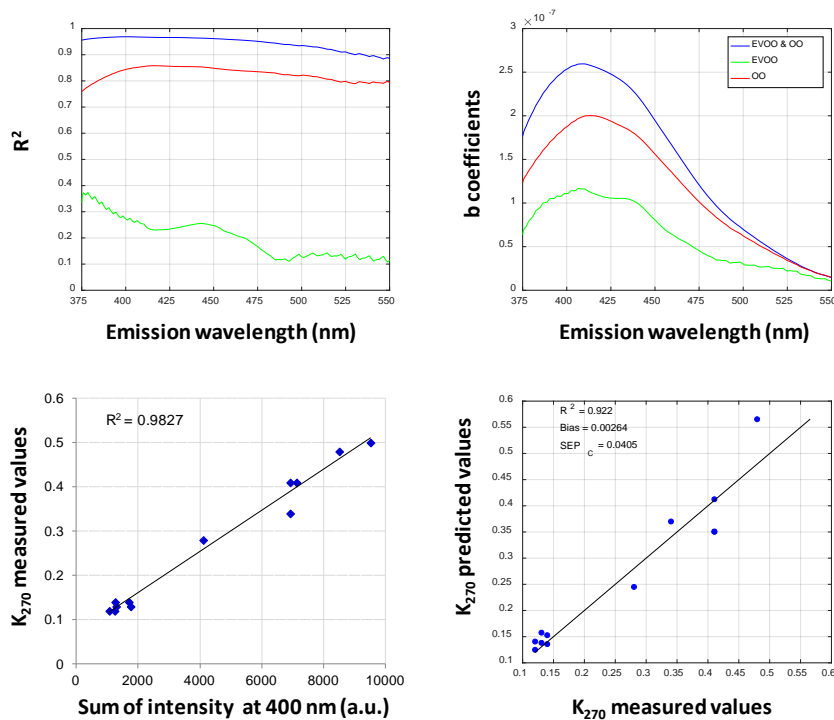


Figure 2. Upper left: coefficient of determination R^2 between the signal intensity at each individual wavelength from 275 to 550 nm and the analytical K_{270} values. Bottom left: intensity of the sum of emission signal at 400 nm versus measured K_{270} values. Upper right: b-coefficients of a PLSR. Bottom right: measured K_{270} values versus predicted K_{270} values by a PLSR (one latent variable) (SEP_c, bias corrected standard error of prediction).

At control month spectra were dominated by the signals from chlorophyll at around 670 nm and the shoulder at 725 nm (Figure 3). After two months, considerable decrease was observed. Opposite evolution was observed for the peaks within the region of oxidation products. Noticeable increase was detected for peaks with local maxima at around 400 nm, 434-437 nm, 464-469 nm, and 510-518 nm (Figure 3). Such peaks were in accordance with those found in FF experiments. PC1 loadings in Figure 3 illustrate the variability. Modelling this evolution with regard to official EVOO samples is the following stage that will be faced.

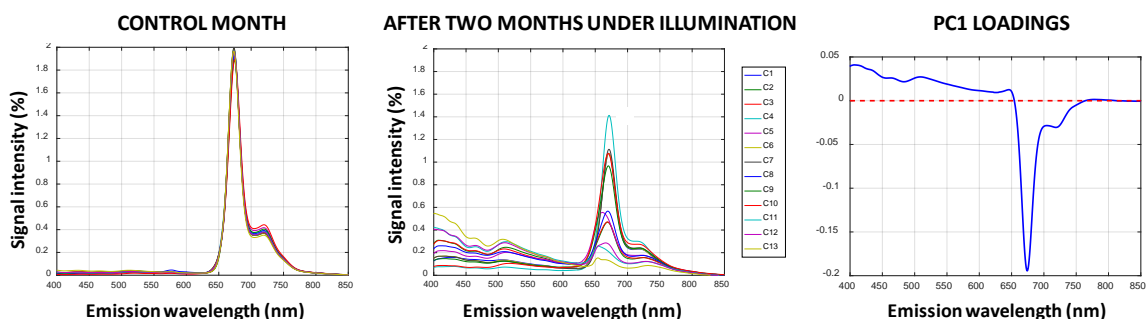


Figure 3. Right-angle fluorescence emission spectra of the commercial EVOO samples. Left: at the control month. Middle: after two months exposed to indirect light. Right: loadings of the first principal component (96.52% explained variance).

Hyperspectral vision

Spectral patterns were established for each maturity stage according to increasing levels of ripening stage: G1 green olives, G1 'pintonas' olives, G2 purple olives, G3 black olives (Figure 4). Green spectra showed a relevant absorption band at 680 nm, corresponding to high chlorophyll content, and high reflectance level at 550 nm, probably related to low anthocyanin content. Average spectrum of 'pintonas' olives and of purple olives, showed similar pattern. It seems that these two types of spectra belonged to the same ripening level. These spectra also showed an absorption band at 680 nm, with lower intensity in comparison to green olives spectra. In addition the intensity of reflectance at 550 nm is lower probably due to higher anthocyanin content. 'Pintonas' olives showed therefore two types of spectra, two different levels of ripening stage within the surface of the fruit. Hyperspectral images are able to sense these differences in comparison to classical spectroscopy measurements, reflecting non-homogeneities of ripening within the surface of the fruit. Finally black spectra showed no absorption band at 680 and no reflectance at 550 nm, suggesting a total degradation of the chlorophyll and high content of anthocyanins respectively.

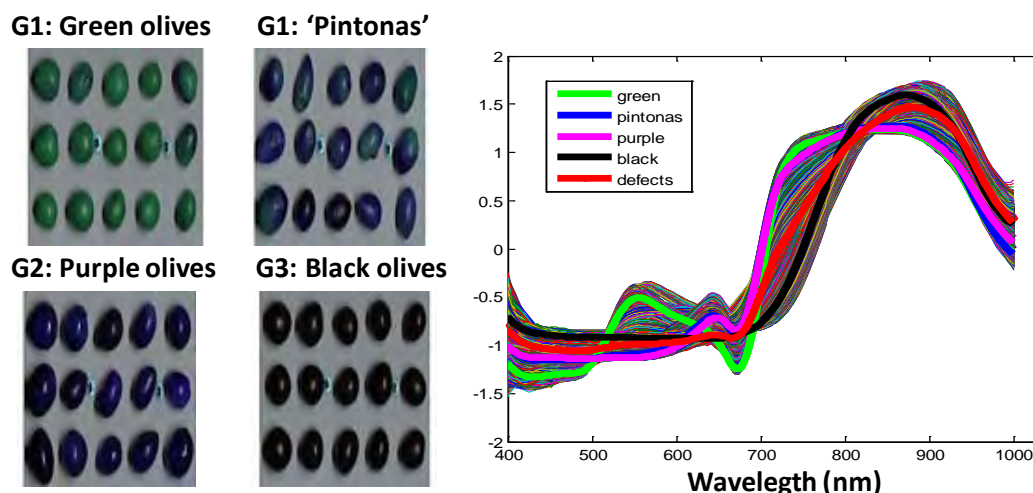


Figure 4. Left: Example of images of olives samples in false colour, merging three colour planes: blue, 450 nm; green, 550; red, 680 nm. Right: Whole set of pre-processed spectra (N=13500); average spectrum of each maturity class is plotted.

CONCLUSIONS

The 3D front-face spectra reveal detailed excitation-emission regions. The coefficient of variation of the signal highlights broad regions related to oxidation processes of olive oil.

The emission band from 375 to 550 nm includes signals produced by an excitation band from 274 nm to 400 nm that shows correlation to the characteristic K_{240} , which is identified with advanced oxidation status. Univariate and multivariate approaches provide correlation with this single parameter.

Simultaneous excitation with a wide range of wavelengths below 400 nm in right-angle experiments is a fast procedure to obtain signals arising from most of the fluorophores related to the complex oxidation processes. The pattern of the spectra acquired using a right-angle device is in accordance with the pattern of the spectra obtained by integrating the emission signal in FF spectra, showing similar positions of the emission peaks.

The right-angle emission spectral pattern of olive oils exposed to illumination evolves to lower chlorophyll signal and to higher signal of oxidation by-products.

Ongoing research highlights that hyperspectral images provide spectral patterns of the olives allowing a more precise sorting into categories, which would enable the classification into lots of oils with more homogeneous characteristics for subsequent modelling.

ACKNOWLEDGMENTS

Authors gratefully acknowledge the Centro Tecnológico Agroalimentario de Lugo (Spain), Comunidad de Madrid (S2013/ABI-2747, TAVS-CM, Spain) and European Structural Funds for financial support. In addition authors gratefully acknowledge Juan Ramón Izquierdo from the Laboratorio Arbitral Agroalimentario of MAGRAMA (Spain) for expertise advice on olive oil quality, and for providing samples and analytical data. LPF-TAGRALIA is part of the CEI Moncloa Campus of Excellence, UPM-UCM (Spain).

Literature cited

- Guzmán, E., Baeten, V., Fernández Pierna, J.A., García-Mesa, J.A. (2015). Evaluation of the overall quality of olive oil using fluorescence spectroscopy. *Food Chemistry*, *173*, 927–934.
- Kyriakidis, N.B., and Skarkalis, P. (2000). Fluorescence spectra measurement of olive oil and other vegetable oils. *Journal of AOAC International*, *83*, 1435–1439.
- Lara, M.A., Lleó, L., Diezma, B., Roger, J.M. and Ruiz-Altisent, M. (2013). Monitoring spinach shelf-life with hyperspectral image through packaging films. *Journal of Food Engineering*, *119*, 383-361. <http://dx.doi.org/10.1016/j.jfoodeng.2013.06.005>.
- López-Miranda, J., F. Pérez-Jiménez, F., Ros, E., De Caterina, R., Badimón, L., Covas, M.I. et al. (2010). Olive oil and health: Summary of the II international conference on olive oil and health consensus report, Jaén and Córdoba (Spain) 200. *Nutrition, Metabolism and Cardiovascular Diseases*, *20* (4), 284–294.
- Lleó, L., J.M. Roger, A. Herrero-Langreo, B. Diezma, P. Barreiro. 2011. Comparison of multispectral indexes extracted from hyperspectral for the assessment of fruit ripening. *Journal of Food Engineering*, *104*, 612-620. [doi:10.1016/j.jfoodeng.2011.01.028](https://doi.org/10.1016/j.jfoodeng.2011.01.028).
- Sikorska, E., Khmelinskii, I., Sikorski, M. (2012). *Analysis of Olive Oils by Fluorescence Spectroscopy: Methods and Applications*, Olive Oil - Constituents, Quality, Health Properties and Bioconversions, Dr. Dimitrios Boskou (Ed.), ISBN: 978-953-307-921-9, InTech, Available from: <http://www.intechopen.com/books/olive-oil-constituents-quality-health-properties-and-bioconversions/analysisof-olive-oils-by-fluorescence-spectroscopy-methods-and-applications>.